

Sea surface temperature records of core ZY2 from the central mud area in the South Yellow Sea during last 6200 years and related effect of the Yellow Sea Warm Current

WANG LiBo^{1,2}, YANG ZuoSheng^{2,*}, ZHANG RongPing³, FAN DeJiang², ZHAO MeiXun³ & HU BangQi^{1,2}

¹ Key Laboratory of Marine Hydrocarbon Resources and Environmental Geology, Ministry of Land and Resources, Qingdao Institute of Marine Geology, Qingdao 266071, China;

² Key Laboratory of Submarine Geosciences and Prospecting Techniques, Ministry of Education, College of Marine Geosciences, Ocean University of China, Qingdao 266100, China;

³ Key Laboratory of Marine Chemistry Theory and Technology, Ministry of Education, College of Chemistry and Chemical Engineering, Ocean University of China, Qingdao 266100, China

Received October 13, 2010; accepted February 17, 2011; published online April 13, 2011

Sea surface temperature (SST) records in the South Yellow Sea during the last 6200 years are reconstructed by the unsaturation index of long-chain alkenones (U_{37}^K) in sediment core ZY2 from the central mud area. The SST records varied between 14.1 and 16.5°C (15.6°C on average), with 3 phases: (1) A high SST phase at 6.2–5.9 cal ka BP; (2) A low and intensely fluctuating SST phase at 5.9–2.3 cal ka BP; and (3) A high and stable SST phase since 2.3 cal ka BP. Variation of the SST records is similar to intensity of the Kuroshio Current (KC), and corresponds well in time to global cold climate events. However, the amplitude of the SST response to cooling events was significantly different in different phases. The SST response to global cooling event was weak while the KC was strong; and the SST response was strong while the KC was weak. The difference in amplitude of the SST response is possibly caused by the modulation effect of the Yellow Sea Warm Current which acts as a shelf branch of the KC and a compensating current induced by the East Asia winter monsoon. The warm waters brought by the Yellow Sea Warm Current cushion the SST decrease induced by climate cooling, and both the Kuroshio and East Asian winter monsoon play important roles in the modulation mechanism. The SST records display a periodicity of 1482 years. The same period was found in the KC records, indicating that variation of the SST records in the central South Yellow Sea is strongly affected by KC intensity. The same period was also found in Greenland ice cores and North Atlantic and Arabian Sea sediment cores, showing a regional response of marine environmental variability in the East China Seas to that in the global oceans.

South Yellow Sea, U_{37}^K , sea surface temperature, Yellow Sea Warm Current, Kuroshio Current, climate change

Citation: Wang L B, Yang Z S, Zhang R P, et al. Sea surface temperature records of core ZY2 from the central mud area in the South Yellow Sea during last 6200 years and related effect of the Yellow Sea Warm Current. Chinese Sci Bull, 2011, 56: 1588–1595, doi: 10.1007/s11434-011-4442-y

The East China Seas (ECSs), including the Bohai Sea, the Yellow Sea and the East China Sea, are to the east of Mainland China, and open to the western Pacific Ocean (Figure 1). They cover one of the world's shallowest and broadest continental shelves, the East China shelf, which

has an area of 9.4×10^5 km² and an average water depth of 56 m inside the edge of the 150 m water depth contour. The Yellow Sea is semi-closed by Mainland China and the Korean Peninsula. The Shandong Peninsula divides the Yellow Sea into two parts, the North and South Yellow Seas. The North Yellow Sea borders the Bohai Sea by the Bohai Strait. The South Yellow Sea (SYS) borders the East China

*Corresponding author (email: zshyang@ouc.edu.cn)

Sea by a line connecting the northern edge of the Yangtze River mouth with Cheju Island, and indirectly opens to the western Pacific Ocean in the south via the East China Sea.

Two of the world's largest rivers in terms of sediment load, the Huanghe (Yellow River) and Changjiang (Yangtze River), discharge about 1.6 billion tons of sediment annually to the ECSs from Mainland China, contributing about 10% of the world's annual sediment discharge [1,2]. During the last deglacial cycle, the ECSs underwent dramatic environmental changes such as eustatic sea-level fluctuation and evolution of cross-shelf circulation system. The cross-shelf circulations are primarily composed of warm, saline oceanic currents and cold, less saline coastal currents (Figure 1). The former mainly consist of the Kuroshio Current (KC), the Tsushima Warm Current (TSWC), the Taiwan Warm Current (TWWC) and the Yellow Sea Warm Current (YSWC); the latter are mainly composed of the Shandong Coastal Current (SDCC), the Jiangsu Coastal Current (JSCC), the Korea Coastal Current (KCC) and the East China Sea Coastal Current (ECSCC) [3–6].

A series of mud patches have developed in the ECSs since the last deglaciation. Grain-size of bulk sediments and quartz isolated from bulk sediments in these mud deposits has been successfully used as a proxy to reconstruct strength changes of the East Asian winter monsoon, because key grain-size component changes induced by coastal currents are closely related to the East Asian winter monsoon [7–12]. These studies document that these mud deposits in the ECSs are valuable for high-resolution Holocene paleo-environmental reconstruction, because of their high sedimentation rates and continuous sedimentation records.

The unsaturation index of long-chain alkenones ($U_{37}^{K'}$) is a good proxy to reconstruct the sea surface temperature (SST), and has been widely used in oceans globally [13–20], including the ECSs [21,22]. The KC, which acts as the western boundary current of Pacific Ocean, plays key role in hydrographic environment of the ECSs by its shelf branch currents. However, their high-resolution shelf sedimentation records have rarely been studied to reconstruct marine environmental responses of ECSs to the KC. The YSWC, a branch current of the KC, flows northward across the central mud area in the SYS and its high temperature characteristic will be recorded in the mud. The SST, which can be reconstructed using the proxy of $U_{37}^{K'}$ of sediments in the central mud area, will indicate environmental responses of the Yellow Sea to the KC via the YSWC, and also indicate the responses to climate changes.

In this study, we analyze the unsaturation index of long-chain alkenones of an AMS ^{14}C dated piston core ZY2, which is located on the path of Yellow Sea Warm Current. We use this to reconstruct the sea surface temperature and discuss the marine environmental responses to the Kuroshio Current and climate changes in the central SYS.

1 Materials and methods

Piston core ZY2 (35°31'N, 122°39'E) was collected in the central mud area in the SYS (Figure 1), at a water depth of 69 m, having a length of 342 cm. Sediments of the core were sampled in the laboratory, at 1 cm intervals.

Samples for grain-size analysis were spaced at 1 cm interval. After pre-treated with 10% H_2O_2 solution to remove organic matter and with 3 mol/L HCl solution to remove carbonate components, grain-sizes of the sediment samples were measured using a Britain Malvern 2000 grain-size analyzer, with a measurement range of 0.02–2000 μm , size resolution of 0.01 Φ and measuring error of less than 3%.

For alkenone analysis, samples were spaced at 2 cm intervals in the top 36 cm of the core and at 4 cm intervals below that depth. About 2 g of freeze-dried sediment was extracted ultrasonically four times with ultra-clean solvents (dichloromethane/methanol, 3/1 by vol.), after adding the C_{24} deuterium-substituted *n*-alkane and C_{19} alcohol as internal standard. The extracts were hydrolyzed in KOH-MeOH solution, and then separated by silica gel cartridges.

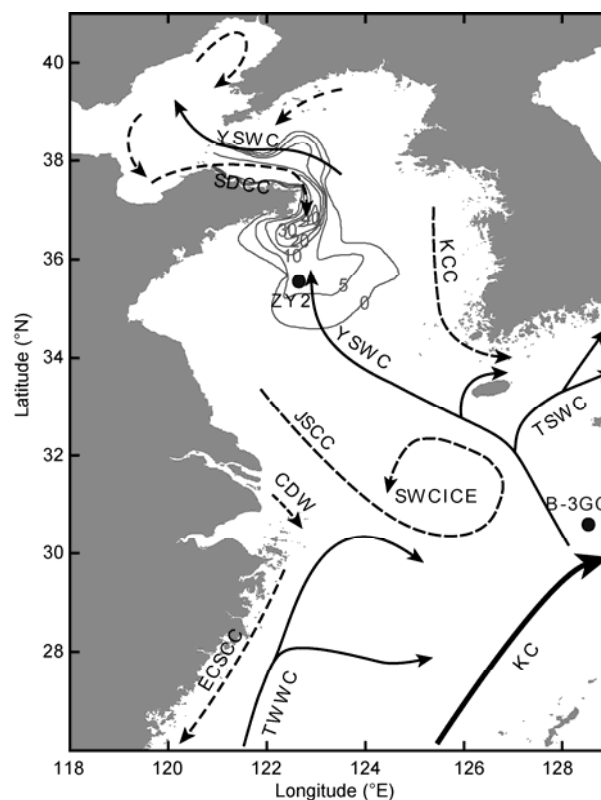


Figure 1 Location of core sites, Holocene sediment thickness off the Shandong Peninsular [23] (gray lines) and winter circulations in the ECSs [24]. The circulations include: YSWC, Yellow Sea Warm Current; TSWC, Tsushima Current; TWWC, Taiwan Warm Current; KC, Kuroshio Current; SDCC, Shandong Coastal Current; JSCC, Jiangsu Coastal Current; KCC, Korea Coastal Current; ECSCC, East China Sea Coastal Current; CDW, Changjiang Diluted Water; SWCICE, Southwestern Cheju Island Cold Eddy.

After derivatization by N,O-Bis(trimethylsilyl)trifluoroacetamide (BSTFA), alkenones within the alcohol subfraction were analyzed by gas chromatography. Biomarker identification and structure verification were performed on a Thermo Gas Chromatography/Mass Spectrometry. Quantification of the biomarkers was done on an Agilent 6890N gas chromatography, using a HP-1 column (50 m), H₂ as carrier gas at 1.2 mL/min. SST was calculated using the following equation [25]: $SST = (U_{37}^{K'} - 0.044) / 0.033$, which is suitable for ECSs [22].

Mixed benthic foraminifera were used for AMS ¹⁴C dating, performed in the Accelerator Mass Spectrometry Laboratory, Peking University. Raw radiocarbon dates were calibrated by Calib 5.0.2 [26], using Marine04 curve [27], setting the difference in reservoir age (ΔR) between the local region and the model ocean to zero (Table 1).

2 Results

2.1 Lithology and chronology

Lithology of core ZY2 is homogeneous and mainly composed of grey, dark grey clay silt from the top down, with mean grain-size between 7.03 to 7.67 Φ (7.42 Φ on average). Grain-size distribution curves of the sediments are unimodal, indicating a stable sedimentary environment. The core has no sedimentation hiatus; sedimentation rates were 44 to 101 cm/ka based on AMS ¹⁴C data (Figure 2). Calendar age at the bottom layer of the core is about 6.2 cal ka BP. Because of sample measurement intervals, resolutions of grain-size time series of core ZY2 are about 18 years. Resolutions for SST are about 36 years in the top 36 cm of the core and 72 years below that depth.

2.2 Sea surface temperature

During the past 6.2 cal ka BP, the $U_{37}^{K'}$ -SST of core ZY2 in the central SYS fluctuated between 14.1–16.5°C, 15.6°C on average (Figure 3), similar to the results of nearby core YE2 [21]. The SST time series can be divided into three phases: the SSTs were high from 6.2 to 5.9 cal ka BP, fluctuating between 15.8–16.2°C, 16.1°C on average; the SSTs were low from 5.9 to 2.3 cal ka BP, intensely fluctuating between 14.1–16.0°C, 15.2°C on average; the SSTs were high and stable from 2.3 to 0 cal ka BP, fluctuating between 15.3 to 16.5°C, 15.9°C on average. Three prominent low SST intervals occurred at 5.5–5.05, 4.0–3.75 and 3.0–2.4 cal ka BP, when the SSTs were less than 15°C.

Spectral analysis of the $U_{37}^{K'}$ -SST time series of core ZY2 was performed using the software REDFIT35, which is programmed for spectral analysis of an unevenly spaced time series [28]. Settings were: n50=4; Welch spectrum windows; remaining parameters as default. The result shows the highest confidence level period of 1482 years (Figure 4). This period is closely related to oceanic thermohaline circulation, and exists in the KC [29], Greenland ice core [30], North Atlantic sediments [31,32] and Arabian Sea sediments

Table 1 AMS ¹⁴C age data of core ZY2

Depth (cm)	AMS ¹⁴ C age (a BP)	Calendar age (cal a BP)	2 σ error bars (cal a BP)
67.5	1825±30	1360	1287–1457
128.5	2345±40	1964	1861–2089
237.5	3955±40	3947	3831–4072
272.5	4450±45	4633	4499–4792
329.5	5555±40	5941	5857–6082

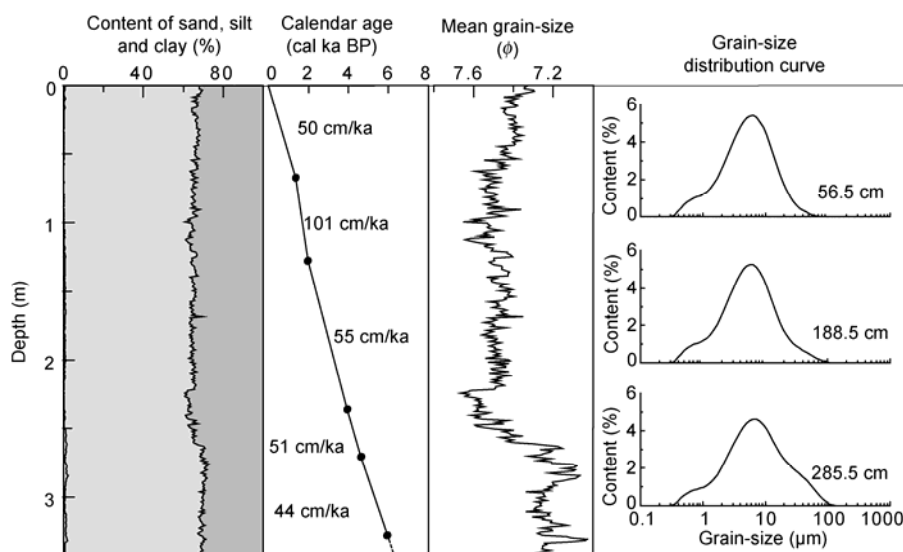


Figure 2 Variation of lithology, grain size and age model in core ZY2. The lithology is homogeneous, with sand content less than 1%, silt content about 65% and clay content about 35%. Grain-size distribution curves are unimodal. Sedimentation rates are 44 to 101 cm/ka.

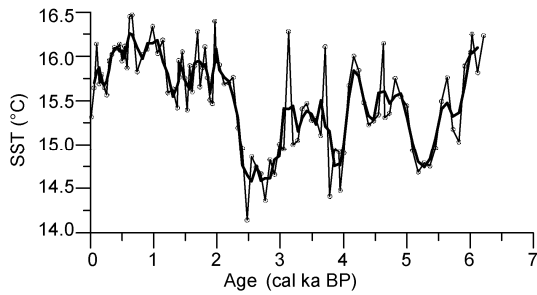


Figure 3 U_{37}^{K1} -SST time series (thin line) and three points moving average (thick line) in core ZY2.

[33], suggesting there is a marine environmental tele-connection between the East China Seas and global oceans.

3 Discussion

3.1 Response of the SST to climate event

The SST variations in the central SYS during the past 6.2 cal ka BP, show a good correspondence to global/regional climate events, especially the three prominent low SST intervals (5.5–5.05, 4.0–3.75 and 3.0–2.4 cal ka BP).

The East Asian monsoon is an important factor influencing the SST. Weakening of summer monsoon or intensification of winter monsoon may decrease the SST in the central SYS. Desiccation of the Taiwan Retreat Lake between 4.5 and 2.1 cal ka BP and reduction of its TOC content between 5.8 and 5.1 cal ka BP indicate summer monsoon weakening in these periods [34,35], which is consistent with the three low SST intervals (Figure 5b). Magnetic susceptibility and Ti content of the Lake Huguang Maar sediments suggest winter monsoon intensification in these three intervals [36]. Additionally, studies of the Dunde ice core [37,38], Hongyuan peat [39] and historical documents [40,41] demonstrate climate cooling in the three low SST intervals.

The SST variations are closely related to cold climate events recorded by the Greenland ice core and North Atlantic sediments. Increases of sea salt and terrestrial dust content of the Greenland ice core GISP2 at 6100–5000, 4000–

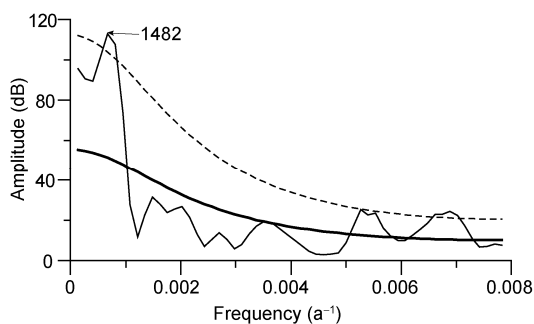


Figure 4 Spectrum of SST time series (thin solid line), theoretical red-noise spectrum (thick solid line) and false-alarm level of 95% (dash line). The result shows a period of 1482 years.

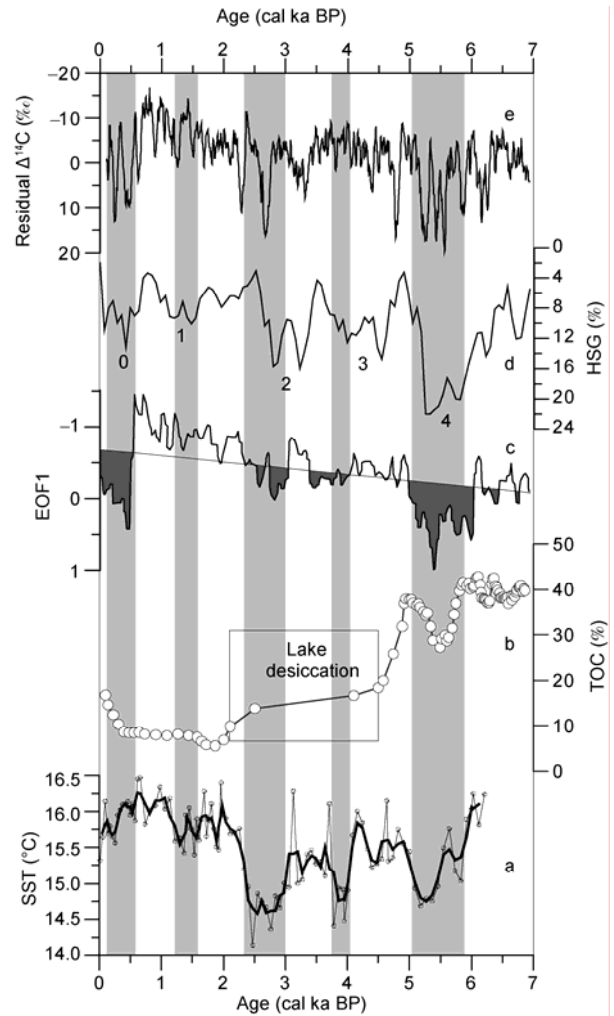


Figure 5 Comparison of SST in the central SYS with cold climate events. a, SST time series (thin line) and three points moving average (thick line) in core ZY2; b, TOC content in Taiwan Retreat Lake sediment core [34,35]: low content and lake desiccation indicates weak East Asian summer monsoon; c, EOF1 proxy in Greenland ice core GISP2 [30]: high EOF1 indicates climate cooling; d, percentage of hematite-stained grains (HSG) in North Atlantic deep sea cores MC52-VM29-191 [31,32]: high percentage peaks indicate four cold climate events in the past 6000 years; e, atmospheric residual $\Delta^{14}C$ after removing a 2000 years moving average: high value indicates solar irradiance decrease.

3500 and 3100–2400 cal a BP indicate temperature decreases in the mid to high northern latitudes [30], which correspond well to the three low SST intervals (Figure 5c). A series of Holocene cold climate events have been identified from North Atlantic deep sea cores [31,32], and the three low SST intervals correspond to the Bond ice rafted debris events 2, 3 and 4 (Figure 5d).

Relationships of the SST variations in the central SYS to Holocene glacier and solar activity are significant. Denton and Karlén [42] proposed several intervals of Holocene glacier expansion. Two of these intervals, in 5800–4900 and 3300–2400 cal a BP, correspond to the low SST intervals in 5.05–5.5 and 3.0–2.4 cal ka BP respectively. Increase of residual $\Delta^{14}C$ during 5.05–5.5 and 3.0–2.4 cal ka BP intervals

indicate reduction of solar irradiance [43], consistent with the SST decrease (Figure 5e).

The SST variations in the central SYS are also linked to warm climate. The Sui-Tang Warm Period (1380–1180 cal a BP) in China and Medieval Warm Period (1050–650 cal a BP) in Europe occurred during the interval of 2.3–0 cal ka BP, when the SST was relative high. However, the short high SST interval of 6.2–5.9 cal ka BP is possibly influenced by the intrusion of YSWC, because the SSTs increased intensively at the beginning of the YSWC intrusion [21].

3.2 Response of the SST to the Kuroshio Current

The YSWC, which brings warm and saline waters from southwest of Cheju Island to the Yellow Sea and forms warm and saline tongue structures in winter, is an important member of the cross-shelf circulations and plays a key role in water exchange and evolution of marine environments in the Yellow Sea. It has been proposed that the YSWC was formed at 6.5 cal ka BP [21], 6.4 cal ka BP [44,45] or 6 cal ka BP [46]. Core ZY2 is located on the front of YSWC influenced area, and age at the bottom of the core is 6.2 cal ka BP, so that sedimentary records after the intrusion of YSWC may be preserved in the core. If the YSWC intensifies, the warm tongue will extend further north and bring more warm water, causing an increase of the SST in the position of core ZY2, and vice versa. According to SST along the 36° N transect in the Yellow Sea in February from 1985–2007 [47], which is calculated to indicate northward extension intensity of the YSWC, discrepancies in transect mean temperatures in different years are mostly greater than 2°C.

Physical oceanographic studies reveal that northward extension of the YSWC is closely related to the KC [47,48]. About 2/3 of the annual mean YSWC transport is mainly determined by the KC, another 1/3 is mainly determined by the local wind [48]. Core B-3GC, which is taken from northern Okinawa Trough, is located in the root of the warm tongue that extends to the Yellow Sea. This is close to the source of YSWC, and influenced by the TSWC, which is a branch of the KC (Figure 1). Core ZY2 is located in the front of the warm tongue (Figure 1). Comparison between the two cores will reveal the influence of the KC on core ZY2 (Figure 6). The general trend of the SST variation in core ZY2 (Figure 6a) is consistent with that of the abundance (Figure 6b) and $\delta^{18}\text{O}$ (Figure 6c) of *P. obliquiloculata* (an indicator species of the KC) in core B-3GC [29], considering the chronological uncertainty of the two cores. The SST derived from core ZY2 increases while the KC influence intensifies, but decreases while the KC weakens. The *P. obliquiloculata* minimum event during 4.6–2.7 cal ka BP, for example, shows that the SST from core ZY2 decreases while the KC influence weakens. The reason for this relationship is that weakening of the KC will reduce the

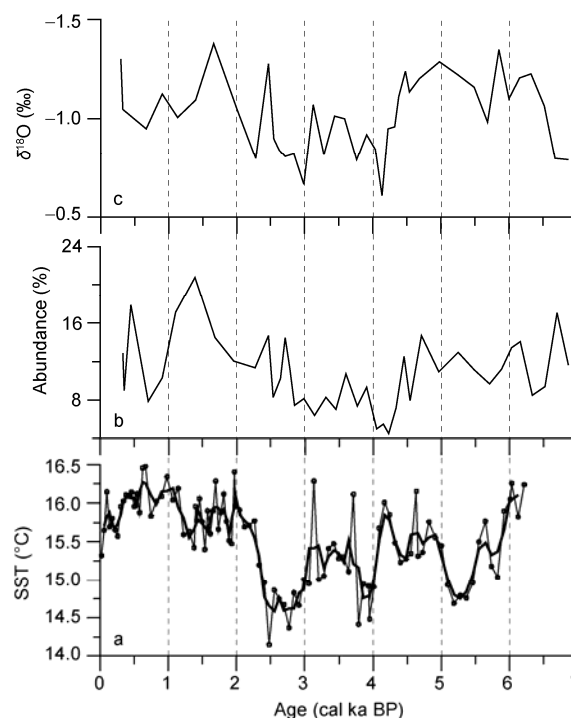


Figure 6 Comparison of SST in the central SYS with KC proxies. a, SST time series (thin line) and three points moving average (thick line) in core ZY2; b, abundance; c, $\delta^{18}\text{O}$ of *P. obliquiloculata* (an indicator species of the KC) in core B-3GC [29].

YSWC. Subsequent reduction of northward extension of the warm tongue will decrease the SST in the sea area near core ZY2. However, strengthening of the KC will intensify the YSWC, increasing northward extension of the warm tongue, which will increase the SST in the sea area near core ZY2. The correlation indicates that the SST variations in the central SYS, which are influenced by the YSWC, respond well to the KC variations.

3.3 Modulation effect of the Yellow Sea Warm Current to the SST

During the Little Ice Age (600–150 cal a BP [49]), which was a pervasive cold interval in global climate changes, climate proxies fluctuated intensively (Figure 5c–e). Chinese historical documents [41,50–52] showed that temperatures in eastern China at that time were the coldest in the past 2000 years. However, the SST decreased gently, with only low amplitude. The cold climate event at 1.4 cal ka BP recorded by the North Atlantic sediments [31,32] is also not obvious in the SST time series of core ZY2 (Figure 5a,d). As shown in Figure 5c–e, amplitudes of cold climate events in 3.0–2.4 and 4.0–3.75 cal ka BP were less than that in 5.5–5.05 cal ka BP, but decrease of the SST in the first two intervals was greater than that in the last interval (Figure 5a). By comparison with the KC indicators (Figure 6b, c), the amplitude of the SST decrease in the central SYS in response to the global/regional cold climate events was low

and the response was weak when the KC was strong, but the amplitude was high and the response strong when the KC was weak.

One reason for the amplitude discrepancy between SST decrease and climate cooling may be a modulation effect of the YSWC to the SST. The YSWC, which is a compensation flow induced by the northerly wind [53,54], is not only influenced by the KC [47,48], but also influenced by the East Asian winter monsoon [6,53,55,56]. Strong northerly wind will cause the YSWC to extend further northward [53,55,56] and shift westward [6,47,56], bringing the axis of the YSWC closer to the location of core ZY2 (Figure 1). That is to say, if the KC and East Asian winter monsoon intensify, the YSWC will bring more warm water to the sea area near core ZY2.

During the Little Ice Age, the KC and East Asian winter monsoon were both strong [7–9,29,36]. Combination of these two factors led the YSWC to intensify because of its dual properties of compensation flow induced by the winter monsoon and shelf branch flow of the KC [6,47,48,53,55,56]. Therefore, more warm water at the back of the YSWC transported northward. At the same time, strong winter monsoon caused the axis of the YSWC to shift westward [6,47,56], bringing it closer to core ZY2 (Figure 1). SST increase in the central SYS induced by northward extension and westward shift of the YSWC, largely negated the influence of climate cooling to cause SST decrease, making the amplitude of SST reduction in the Little Ice Age relatively small. The strong KC [29] around 1.4 cal ka BP (Figure 6b, c) intensified the YSWC; warm water which extended northward partly negated the influence of climate cooling to decrease SST, similar to circumstances during the Little Ice Age. Additionally, amplitude of the 1.4 cal ka BP cold event seems not particularly high (Figure 5c–e). During 3.0–2.4 cal ka BP, amplitude of climate cooling was lower than that in the 5.5–5.05 cal ka BP interval (Figure 5c–e). However, the weak KC and winter monsoon [29,36] (Figure 6b, c) caused the YSWC to be weak, so less warm water at the back of the YSWC transported northward, largely reducing the negating effect of the YSWC to SST decrease induced by climate cooling. Therefore, amplitude of the SST decrease in the 3.0–2.4 cal ka BP was highest. Circumstances during 4.0–3.75 cal ka BP were similar to those in the 3.0–2.4 cal ka BP interval. During 5.5–5.05 cal ka BP, the KC was slightly weak [29] (Figure 6b, c), but the winter monsoon was very strong [36], still causing the YSWC to extend northward and shift westward, and partly negating the SST decrease induced by climate cooling. Therefore, although amplitude of climate cooling during 5.5–5.05 cal ka BP interval was higher than that in 3.0–2.4 cal ka BP interval (Figure 5c–e), amplitude of SST decrease in the former interval was less than that in the latter interval.

The YSWC, which has dual properties of compensation flow induced by the East Asian winter monsoon and shelf branch flow of the KC, significantly influences marine en-

vironments of the ECSs, and modulates responses of SST to climate changes (especially short duration cold climate events) in the central SYS. The modulation mechanism is that the strong KC and winter monsoon will intensify the YSWC, bringing more warm water to the central SYS and negating SST decrease induced by climate cooling in the central SYS; weak KC and winter monsoon have the opposite effect. The KC and winter monsoon are key factors that influence intensity of the YSWC, and play key roles in the modulation mechanism.

4 Conclusions

(1) Based on the unsaturation index of long-chain alkenones ($U_{37}^{K'}$) in core ZY2, SST in the central SYS during the past 6200 years fluctuated between 14.1 and 16.5°C (15.6°C on average), similar to findings of previous studies [21]. Temperatures were high during 6.2–5.9 cal ka BP, were low and fluctuated intensely during 5.9–2.3 cal ka BP and were high and stable during 2.3–0 cal ka BP. The SST time series are interspaced with three low SST (<15°C) intervals at 5.5–5.05, 4.0–3.75 and 3.0–2.4 cal ka BP. Spectral analysis shows a period of 1482 years existing in the SST variations.

(2) SST variations in the central SYS recorded by core ZY2 correspond well to the global climate changes and KC variations. The SST variations are generally consistent with the KC variations. Amplitude of SST response to a cold climate event is significantly different in different KC variation phases. Generally, the SST response to a global/regional cooling event is weak while the KC is strong, and the SST response is strong while the KC is weak.

(3) The reason for the amplitude discrepancy between SST decrease and climate cooling may be the modulation effect of the YSWC. Warm water brought by the warm current will negate SST decrease induced by climate cooling. The YSWC has dual properties of compensation flow induced by the East Asian winter monsoon and shelf branch flow of the KC. Therefore, strong KC and winter monsoon will intensify the YSWC, bringing more warm water to the central SYS. Then, the negating effect to SST decrease will be intensified, and vice versa. Both the intensity of KC and the variation of East Asian winter monsoon play key roles in the modulation mechanism.

The authors would like to thank Dr. Liu Yanguang from the Key Laboratory of Marine Sedimentology and Environmental Geology, State Oceanic Administration for the help with grain-size analysis, Zhang Hailong from Ocean University of China for the help with biomarkers analysis, and two anonymous reviewers for their valuable comments that considerably improved the manuscript. This work was supported by the National Basic Research Program of China (2010CB428901) and the National Natural Science Foundation of China (90211022 and 41020164005).

- 1 Milliman J D, Meade R H. World-wide delivery of river sediment to the oceans. *J Geol*, 1983, 91: 1–21

- 2 Milliman J D, Syvitski J P M. Geomorphic/tectonic control of sediment discharge to the ocean: The importance of small mountainous rivers. *J Geol*, 1992, 100: 525–544
- 3 Su J. A review of circulation dynamics of the coastal oceans near China (in Chinese). *Acta Oceanol Sin*, 2001, 23: 1–16
- 4 Zang J, Tang Y, Zou E, et al. Analysis of Yellow Sea circulation. *Chinese Sci Bull*, 2003, 48(Suppl 1): 12–20
- 5 Yuan D, Zhu J, Li C, et al. Cross-shelf circulation in the Yellow and East China Seas indicated by MODIS satellite observations. *J Mar Syst*, 2008, 70: 134–149
- 6 Yuan D, Hsueh Y. Dynamics of the cross-shelf circulation in the Yellow and East China Seas in winter. *Deep-Sea Res Part II*, 2010, 57: 1745–1761
- 7 Qiao S, Yang Z, Liu J, et al. Records of late-Holocene East Asian winter monsoon in the East China Sea: Key grain-size component of quartz versus bulk sediments. *Quat Int*, 2011, 230: 106–114
- 8 Xiao S, Li A, Jiang F, et al. Recent 2000-year geological records of mud in the inner shelf of the East China Sea and their climatic implications. *Chinese Sci Bull*, 2005, 50: 466–471
- 9 Xiang R, Yang Z, Saito Y, et al. East Asia Winter Monsoon changes inferred from environmentally sensitive grain-size component records during the last 2300 years in mud area southwest off Cheju Island, ECS. *Sci China Ser D-Earth Sci*, 2006, 49: 604–614
- 10 Xiao S, Li A, Liu J P, et al. Coherence between solar activity and the East Asian winter monsoon variability in the past 8000 years from Yangtze River-derived mud in the East China Sea. *Paleogeogr Paleoclimatol Paleocol*, 2006, 237: 293–304
- 11 Xu F, Li A, Xu K, et al. Cold event at 5500 a BP recorded in mud sediments on the inner shelf of the East China Sea. *Chin J Oceanol Limnol*, 2009, 27: 975–984
- 12 Liu S, Shi X, Liu Y, et al. Records of the East Asian winter monsoon from the mud area on the inner shelf of the East China Sea since the mid-Holocene. *Chinese Sci Bull*, 2010, 55: 2306–2314
- 13 Prahl F G, Wakeham S G. Calibration of unsaturation patterns in long-chain ketone compositions for palaeotemperature assessment. *Nature*, 1987, 330: 367–369
- 14 Prahl F G, Muehlhausen L A, Zahnle D L. Further evaluation of long-chain alkenones as indicators of paleoceanographic conditions. *Geochim Cosmochim Acta*, 1988, 52: 2303–2310
- 15 Prahl F G, Collier R B, Dymond J, et al. A biomarker perspective on prymnesiophyte productivity in the northeast pacific ocean. *Deep-Sea Res Part I*, 1993, 40: 2061–2076
- 16 Bard E, Rostek F, Sonzogni C. Interhemispheric synchrony of the last deglaciation inferred from alkenone palaeothermometry. *Nature*, 1997, 385: 707–710
- 17 Villanueva J, Grimalt J O, Cortijo E, et al. Assessment of sea surface temperature variations in the central North Atlantic using the alkenone unsaturation index (U_{37}^k). *Geochim Cosmochim Acta*, 1998, 62: 2421–2427
- 18 Zhao M, Eglinton G, Haslett S K, et al. Marine and terrestrial biomarker records for the last 35000 years at ODP site 658C off NW Africa. *Org Geochem*, 2000, 31: 919–930
- 19 Zhao M, Eglinton G, Read G, et al. An alkenone (U_{37}^k) quasi-annual sea surface temperature record (A.D. 1440 to 1940) using varved sediments from the Santa Barbara Basin. *Org Geochem*, 2000, 31: 903–917
- 20 Zhao M, Huang C Y, Wang C C, et al. A millennial-scale U_{37}^k sea-surface temperature record from the South China Sea (8°N) over the last 150 kyr: Monsoon and sea-level influence. *Paleogeogr Paleoclimatol Paleocol*, 2006, 236: 39–55
- 21 Wang L, Yang Z, Zhao X, et al. Sedimentary characteristics of core YE-2 from the central mud area in the South Yellow Sea during last 8 400 years and its interspace coarser layers (in Chinese). *Mar Geol Quat Geol*, 2009, 29: 1–11
- 22 Li G, Sun X, Liu Y, et al. Sea surface temperature record from the north of the East China Sea since late Holocene. *Chinese Sci Bull*, 2009, 54: 4507–4513
- 23 Yang Z S, Liu J P. A unique Yellow River-derived distal subaqueous delta in the Yellow Sea. *Mar Geol*, 2007, 240: 169–176
- 24 Guo B, Xu J. Circulations of the coastal oceans near China. In: Su J, Yuan Y, eds. *Hydrography of the Coastal Oceans Near China* (in Chinese). Beijing: Ocean Press, 2005. 174–182
- 25 Müller P J, Kirst G, Ruhland G, et al. Calibration of the alkenone paleotemperature index U_{37}^k based on core-tops from the eastern South Atlantic and the global ocean (60°N–60°S). *Geochim Cosmochim Acta*, 1998, 62: 1757–1772
- 26 Stuiver M, Reimer P J. Extended ^{14}C database and revised CALIB radiocarbon calibration program. *Radiocarbon*, 1993, 35: 215–230
- 27 Hughen K A, Baillie M G L, Bard E, et al. Marine04 marine radiocarbon age calibration, 0–26 cal kyr BP. *Radiocarbon*, 2004, 46: 1059–1086
- 28 Schulz M, Mudelsee M. REDFIT: Estimating red-noise spectra directly from unevenly spaced paleoclimatic time series. *Comput Geosci-uk*, 2002, 28: 421–426
- 29 Jian Z, Wang P, Saito Y, et al. Holocene variability of the Kuroshio Current in the Okinawa Trough, northwestern Pacific Ocean. *Earth Planet Sci Lett*, 2000, 184: 305–319
- 30 O'Brien S R, Mayewski P A, Meeker L D, et al. Complexity of Holocene climate as reconstructed from a Greenland Ice Core. *Science*, 1995, 270: 1962–1964
- 31 Bond G, Showers W, Cheseby M, et al. A pervasive millennial-scale cycle in North Atlantic Holocene and glacial climates. *Science*, 1997, 278: 1257–1266
- 32 Bond G, Kromer B, Beer J, et al. Persistent solar influence on North Atlantic climate during the Holocene. *Science*, 2001, 294: 2130–2136
- 33 Sirocko F, Garbe-Schönberg D, McIntyre A, et al. Teleconnections between the subtropical monsoons and high-latitude climates during the Last Deglaciation. *Science*, 1996, 272: 526–529
- 34 Selvaraj K, Chen C T, Lou J Y. Holocene East Asian monsoon variability: Links to solar and tropical Pacific forcing. *Geophys Res Lett*, 2007, 34: L01703
- 35 Selvaraj K, Arthur Chen C-T, Lou J Y, et al. Holocene weak summer East Asian monsoon intervals in Taiwan and plausible mechanisms. *Quat Int*, 2011, 229: 57–66
- 36 Yancheva G, Nowaczyk N R, Mingram J, et al. Influence of the intertropical convergence zone on the East Asian monsoon. *Nature*, 2007, 445: 74–77
- 37 Yao T, Thompson L G. Trends and features of climatic changes in the past 5000 years recorded by the Dunde ice core. *Ann Glaciol*, 1992, 16: 21–24
- 38 Shi Y, Kong Z, Wang S, et al. Mid-holocene climates and environments in China. *Glob Planet Change*, 1993, 7: 219–233
- 39 Xu H, Hong Y, Lin Q, et al. Temperature variations in the past 6000 years inferred from $\delta^{18}\text{O}$ of peat cellulose from Hongyuan, China. *Chinese Sci Bull*, 2002, 47: 1578–1584
- 40 Hou Y, Zhu Y. Important climatic events showed by historical records from middle and lower reach plain of the Yellow River during 5–2.7 ka and their environmental significance (in Chinese). *Mar Geol Quat Geol*, 2000, 20: 23–29
- 41 Ge Q, Wang S, Zheng J. Reconstruction of temperature series in China for the last 5000 years. *Prog Nat Sci*, 2006, 16: 838–845
- 42 Denton G H, Karlén W. Holocene climatic variations—Their pattern and possible cause. *Quat Res*, 1973, 3: 155–174
- 43 Stuiver M, Reimer P, Bard E, et al. INTCAL98 radiocarbon age calibration, 24000–0 cal a BP. *Radiocarbon*, 1998, 40: 1041–1083
- 44 Li T, Li S, Cang S, et al. Paleo-hydrological reconstruction of the southern Yellow Sea inferred from foraminiferal fauna in core YSDP102 (in Chinese). *Oceanol Limnol Sin*, 2000, 31: 588–595
- 45 Li T, Jiang B, Sun R, et al. Evolution pattern of warm current system of the East China Sea and the Yellow Sea since the Last Deglaciation (in Chinese). *Quat Sci*, 2007, 27: 945–954
- 46 Liu J, Li S, Wang S, et al. Sea level changes of the yellow sea and formation of the yellow sea warm current since the last deglaciation (in Chinese). *Mar Geol Quat Geol*, 1999, 19: 13–24
- 47 Song D, Bao X, Wang X, et al. The inter-annual variability of the Yellow Sea Warm Current surface axis and its influencing factors.

- Chin J Oceanol Limnol, 2009, 27: 607–613
- 48 Xu L, Wu D, Lin X, et al. The study of the Yellow Sea Warm Current and its seasonal variability. *J Hydrodyn Ser B*, 2009, 21: 159–165
- 49 Stuiver M, Grootes P M, Braziunas T F. The GISP2 $\delta^{18}\text{O}$ Climate Record of the Past 16500 Years and the role of the Sun, ocean, and volcanoes. *Quat Res*, 1995, 44: 341–354
- 50 Zhu K. A preliminary study on the climate changes since the last 5000 years in China (in Chinese). *Sci China*, 1973, 2: 168–189
- 51 Ge Q, Zheng J, Fang X, et al. Winter half-year temperature reconstruction for the middle and lower reaches of the Yellow River and Yangtze River, China, during the past 2000 years. *Holocene*, 2003, 13: 933–940
- 52 Ge Q, Zheng J, Fang X, et al. Temperature changes of winter-half-year in eastern China during the past 2000 years (in Chinese). *Qua Sci*, 2002, 22: 166–173
- 53 Naimie C E, Blain C A, Lynch D R. Seasonal mean circulation in the Yellow Sea—A model-generated climatology. *Cont Shelf Res*, 2001, 21: 667–695
- 54 Tang Y. Circulations of the Yellow Sea. In: Su J, Yuan Y, eds. *Hydrography of the Coastal Oceans Near China* (in Chinese). Beijing: Ocean Press, 2005. 200–202
- 55 Mask A C, O'Brien J J, Preller R. Wind-driven effects on the Yellow Sea Warm Current. *J Geophys Res*, 1998, 103: 30713–30729
- 56 Tang Y, Zou E, Lie H-J. On the origin and path of the Huanghai Warm Current during winter and early spring (in Chinese). *Acta Oceanol Sin*, 2001, 23: 1–12

Open Access This article is distributed under the terms of the Creative Commons Attribution License which permits any use, distribution, and reproduction in any medium, provided the original author(s) and source are credited.